Distribution of resonance strengths in microwave billiards of mixed and chaotic dynamics

C. Dembowski,[1,*] B. Dietz,[1] T. Friedrich,[1] H.-D. Gräf,[1] H. L. Harney,[2] A. Heine,[1,†] M. Miski-Oglu,[1] and A. Richter[1,‡]
[1]*Institut für Kernphysik, Technische Universität Darmstadt, D-64289 Darmstadt, Germany*
[2]*Max-Planck-Institut für Kernphysik, D-69029 Heidelberg, Germany*
(Received 22 December 2004; published 4 April 2005)

A new measure for statistical properties of the wave function components of quantum systems, the distribution of the product of two partial widths, is introduced. It is tested with data obtained in analog experiments with microwave billiards, where the product of two partial widths equals the resonance strengths in the microwave spectra. The billiards are from the family of the Limaçons, one with chaotic and two with mixed classical dynamics. For completely chaotic systems the partial widths generically obey a Porter-Thomas distribution. We show that in this case the distribution of their product equals a K_0 distribution. While we find deviations of the experimental strength distribution from the K_0 distribution for the billiards with mixed dynamics, the distributions agree perfectly for the chaotic billiard, when taking into account the experimental threshold of detection in the theoretical description. Hence, the strength distribution provides another stringent test for the connection between statistical properties of systems with classical chaotic dynamics and random matrix theory.

DOI: 10.1103/PhysRevE.71.046202 PACS number(s): 05.45.Mt

I. INTRODUCTION

In this work, we investigate the properties of resonance widths in quantum billiards. The resonance widths are related to the wave functions. Their statistical distributions provide information on the system which is complementary to that on spectral fluctuations. Following the famous conjecture by Bohigas, Giannoni, and Schmit [1], certain statistical properties of the eigenvalues and the wave functions have been found to be well described by random matrix theory (RMT) (see, e.g., [2–5]). The RMT behavior has been observed experimentally in several types of quantum systems, such as atoms [6], molecules [7], nuclei [8], solid state systems [9], and even in hadron spectra [10], as well as in macroscopic analogs like microwave resonators [11,12], vibrating quartz blocks and aluminum plates [13], or optical setups [14]. Mixed and integrable systems, on the other hand, do not show this type of universal behavior. A transition from regular to chaotic classical dynamics is typically accompanied by a transition from spectra with uncorrelated energies to spectra with RMT behavior. Recently, intermediate behavior has also been observed for certain nuclear excitations [15,16].

In this article we show (*i*) how chaotic behavior can be identified by the statistical properties of the resonance strengths of a microwave resonator and (*ii*) that this behavior differs from RMT behavior, if the classical dynamic is partially integrable. To this extent, we consider data from our earlier experiments [17–19] with three superconducting microwave resonators of different degrees of chaoticity from the family of the so-called Limaçon billiards [20,21].

The paper is organized as follows: In Sec. II, we describe the experiments with the superconducting microwave billiards. In Sec. III, the RMT prediction for the strength distribution in a completely chaotic microwave billiard is introduced and the data analysis as well as the experimental results are presented. We conclude in Sec. IV.

II. EXPERIMENT

A. Microwave billiards of chaotic and mixed dynamics

The Helmholtz equation for the electric field in cylindric resonators is for a wavelength longer than twice the height of the resonator [22,23] equivalent to the Schrödinger equation of a quantum billiard of corresponding shape. Hence, the eigenvalues and the wave functions of a quantum billiard can be determined experimentally by measuring the resonance frequencies and the electric field strengths in a flat cylindric microwave resonator. This analogy has been succesfully used for more than a decade for the study of quantum chaotic phenomena in two-dimensional billiards, e.g., [11,12]. The experiments have been performed with normal conducting, e.g., [24,25], as well as with superconducting resonators, e.g., [26,27]. While normal conducting devices allow an experimental mapping of eigenfunctions at room temperature, e.g., [25,28,29], superconducting resonators, due to their high quality factors, are a prerequisite for obtaining essentially complete sequences of eigenvalues [12]. Wave function measurements have so far not been possible in superconducting resonators. Nevertheless, information about the wave functions of a billiard can be obtained from the widths and the amplitudes of the measured resonances. Namely, the partial widths related to the emitting and the receiving antennae in the measurement of a spectrum are proportional to the electric field intensity at the positions of the corresponding antennae.

*Present address: d-fine GmbH, D-60313 Frankfurt am Main, Germany.
†Present address: Fraunhofer EMI (Ernst-Mach-Institut), D-79104 Freiburg, Germany.
‡Electronic address: richter@ikp.tu-darmstadt.de

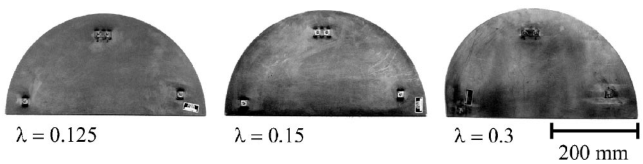

FIG. 1. Photograph of the three desymmetrized Limaçon microwave billiards ($\lambda = 0.125, 0.150, 0.300$). The degree of chaoticity of the corresponding classical billiard has been calculated to 0.55, 0.66, and 1.00, respectively.

In the seminal experiment of [27] the partial widths of the resonances in a chaotic stadium billiard were shown to obey a Porter-Thomas distribution. In the present work we extend these investigations into the regime of mixed classical dynamics, namely, we analyze spectra of microwave billiards (Fig. 1) from the family of the Limaçons [17,18]. These billiards have been used in [17] for the study of the spectral statistics of mixed systems as well as in [18] for a test of trace formulas for chaotic and mixed systems. In the present work we focus on statistical properties of the partial widths.

The boundaries of the investigated billiards are defined as a quadratic conformal map

$$w = z + \lambda z^2 \tag{1}$$

of the unit disk in the complex plane onto the complex plane. The parameter $\lambda \in [0, 1/2]$ controls the degree of chaoticity of the billiard. We investigated Limaçon billiards with parameter values $\lambda = 0.125$, $\lambda = 0.150$, and $\lambda = 0.300$. From a study of the Poincaré surfaces of a section of the corresponding classical dynamics, the fractions of the chaotic phase space were determined to be 0.55, 0.66, and 1.00, respectively [17]. The resonators were manufactured from electron welded niobium sheets, which become superconducting at a critical temperature of approximately 9.2 K [12]. Four antennae are attached to each resonator. The transmission spectra were measured with the help of a HP-8510B network analyzer at a temperature of $T = 4.2$ K—the resonators were cooled down in a liquid helium cryostat—for all six possible antenna combinations (a, b), i.e., for the combinations (1,2), (1,3), (1,4), (2,3), (2,4), and (3,4).

B. Extraction of the resonance parameters

The relative power transmitted from antenna a to antenna b through the cavity

$$\frac{P_{out,b}}{P_{in,a}} \propto |S_{ab}|^2 \quad a \neq b, \tag{2}$$

is proportional to the absolute square of the matrix element S_{ab} of the scattering matrix (S-matrix). It relates the amplitudes of the electromagnetic waves entering channel a to those of the waves exiting via channel b. Close to the frequency f_μ of the μth resonance, the matrix element S_{ab} can be written as

$$S_{ab} = \delta_{ab} - i \frac{\sqrt{\Gamma_{\mu a}\Gamma_{\mu b}}}{f - f_\mu + \frac{i}{2}\Gamma_\mu}. \tag{3}$$

The quantities $\Gamma_{\mu a}$ and $\Gamma_{\mu b}$ are the partial widths related to the antennae a and b; Γ_μ is the total width of the resonance [27]. It is given as the sum of the partial widths $\Gamma_{\mu c}$, $c = 1, 2, 3, 4$, of the four antennae, plus a term which takes into account dissipation in the walls of the superconducting cavity.

For each resonance μ, the transmission measurements provide the product $\Gamma_{\mu a}\Gamma_{\mu b}$ of the partial widths corresponding to the "channels" a and b. *For lack of a better term*, we call this product the strength of the resonance μ with respect to the transmission between the channels a and b. (Note that often the partial width itself is called "strength".) The reader might wonder why we decided to measure the product of two partial widths $\Gamma_{\mu a}\Gamma_{\mu b}$ instead of determining a single partial width directly from a reflection measurement of $|S_{aa}|^2$. There are two reasons. First, in a reflection measurement any additional reflections occurring at the interconnections in the signal paths between the network analyzer and the resonator (e.g., resulting from the microwave feedthroughs of the helium cryostat) make a reliable extraction of the resonance parameters impossible. Second, in a reflection measurement the detected microwave signal results from a fully reflective condition below and above the resonance frequency and is reduced (depending on the coupling strength) across the resonance, whereas in a transmission measurement the detected signal below and above the resonance frequency is the noise floor and a transmitted signal across the resonance exceeding the noise level is easily detected. The resonance strengths are determined by fitting the resonance shape formula given in [30] to the transmission spectra (Eq. (31) in [30]). This formula is slightly more complicated than the so-called Breit-Wigner formula deduced from Eq. (3). Its derivation starts from electromagnetic field conditions of microwave cavities and is based on R-matrix theory [31,32]. It is interesting to note that, while R-matrix theory is a standard theory in nuclear and atomic physics, one of the earliest papers on R-matrix theory [33] uses the object of our investigation—i.e., an electromagnetic resonator—as a prime example.

Our procedure for the extraction of the resonance parameters from the experimental data differs from that used in [27] in two respects. First, even in measurements with the superconducting niobium resonators at a temperature of $T = 4.2$ K there is a significant contribution of losses due to dissipation in the walls to the resonance widths that cannot be neglected. In [27] the losses had been reduced considerably by cooling the system down to $T = 1.8$ K. Second, as already mentioned above, we perform the analysis for transmission spectra. Thus, we cannot measure the individual partial widths but only the products of, respectively, two partial widths [34]. Of course, as the transmission was measured for all combinations of the four antennae, the partial widths can, in principle, be calculated from combinations of the measured products of partial widths. The errors for the deduced partial widths are, however, large. Moreover, the RMT prediction for the distribution of the product of two partial widths may be derived from that for the partial widths themselves. Hence, the investigation of the strength distribution establishes a direct and relatively quick procedure for the study of statistical properties of the wave function components of quantum billiards.

For each of the three resonators six transmission spectra have been analyzed up to a maximum frequency of 20 GHz. The network analyzer was run in a continuous sweep mode with the sweep time set to 0.050 s, where 201 data points were taken in steps of 10 kHz. The resonance frequency f_μ, the total width Γ_μ, and the strength $\Gamma_{\mu a}\Gamma_{\mu b}$ of each resonance μ and each antenna combination (a,b) were determined by proceeding as described in [30,35]. A numerical simulation reveals that the accuracy in the determination of the strength of a resonance is a few percent for a total width of 10 kHz, while it is less than 0.01% for a total width of the order of 40 kHz, which is the typical width of the resonances in the available transmission spectra. Indeed, the theoretical formula for the line shape cannot be fit to some very narrow resonance curves, because the number of data points is insufficient. Moreover, resonances in the transmission spectra with peak heights below a certain value, that is, a very weak electric field at the position of an antenna, may not be detected. However, since the resonance frequency does not depend on the combination of antennae used [see Eq. (3) and the relative uncertainties of the resonance frequencies f_μ given below], an essentially complete sequence of resonance frequencies is obtained by comparing the six transmission spectra.

Individual resonance sequences from a single combination of two antennae are incomplete since resonances may be missed for being either too weakly excited for a particular combination of antennae or being located too close to each other ($\Delta f_\mu \ll \Gamma_\mu$). A careful comparison of the six individual spectra reveals that at most 4% of the resonances are missed in an individual spectrum. We estimate the probability that a resonance is missed in all six transmission spectra to be approximately 10^{-6}, where the correlations between the strengths of the different spectra have been taken into account. An analysis of the nearest-neighbor spacing distribution (NNSD) of the resonance frequencies results in a probability of the order of 10^{-5} for two resonances to be too closely spaced for detection. The probability that one out of 10^3 resonances might have escaped detection is 0.1. This has been verified independently by estimating the expected number of resonances from the geometry of the billiards and Weyl's formula [36,37]. We therefore use the expression "complete" for the resulting sequences of resonances. In this way 1163, 1173, and 946 resonances were identified for the billiards with $\lambda = 0.125$, 0.150, and 0.300, respectively. The strengths depend on the choice of the antennae a and b. Hence, their data sets are incomplete, and, consequently, a threshold of detection has to be taken into account in the theoretical description of the statistical properties of the strengths.

For an illustration of the method of analysis, Fig. 2 shows a transmission spectrum of the $\lambda = 0.300$ billiard obtained for one specific choice of antennae denoted below with $a = 1$, $b = 2$ and three examples of resonances investigated in the present paper. The resonance shape shown in Fig. 2(a) is described by the parameters $f_\mu = (5.834\,272\,51 \pm 6 \times 10^{-8})$ GHz, $\Gamma_\mu = (12.1 \pm 0.4)$ kHz, and $\Gamma_{\mu 1}\Gamma_{\mu 2} = (0.55 \pm 0.03)$ kHz^2, while Fig. 2(c) yields $f_\mu = (6.144\,141\,09 \pm 5 \times 10^{-8})$ GHz, $\Gamma_\mu = (11.4 \pm 0.3)$ kHz, and $\Gamma_{\mu 1}\Gamma_{\mu 2} = (1.18 \pm 0.02)$ kHz^2. Figure 2(b) shows two slightly overlapping resonances. To these a two-level R-matrix formula [30,35] has been fitted. The parameters of the doublet in Fig. 2 are $f_\mu = (6.103\,844\,42 \pm 8 \times 10^{-8})$ GHz, $\Gamma_\mu = (16.5 \pm 0.8)$ kHz, and $\Gamma_{\mu 1}\Gamma_{\mu 2} = (0.48 \pm 0.01)$ kHz^2 for the lower lying resonance and $f_{\mu'} = (6.106\,401\,98 \pm 8 \times 10^{-8})$ GHz, $\Gamma_{\mu'} = (15.2 \pm 0.8)$ kHz, and $\Gamma_{\mu' 1}\Gamma_{\mu' 2} = (0.12 \pm 0.03)$ kHz^2 for the higher lying one.

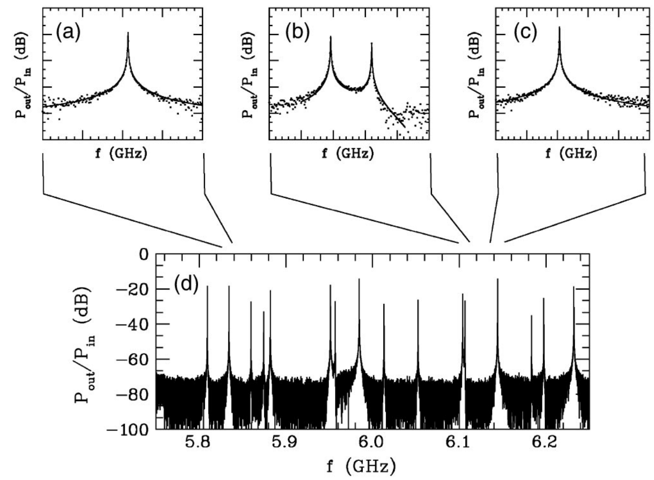

FIG. 2. Part of the transmission spectrum of the superconducting $\lambda = 0.300$ Limaçon microwave billiard. The upper part shows magnifications of the transmission spectrum in the vicinity of two singlets (a) and (c) and a doublet (b). For all three cases the resonance formulas of [30] have been fitted to the measured spectrum.

In Fig. 3 the total widths and, for comparison, the square root of the strengths of the resonances are plotted for one antenna combination of the $\lambda = 0.300$ billiard versus the resonance frequency. They show strong fluctuations around a slow secular variation which is removed before the data are further analyzed by fitting a polynomial of fifth order to the total widths and scaling all widths with this polynomial as in [27].

III. THEORY, ANALYSIS, AND DISCUSSION

According to the Bohigas-Giannoni-Schmit conjecture [1], the statistical properties of a quantum billiard whose classical dynamics is fully chaotic coincide with those of random matrices from the Gaussian orthogonal ensemble (GOE). This implies that the components of the eigenvectors—with respect to any basis—have a Gaussian distribution centered at zero [2]. Accordingly, the partial widths have a χ^2 distribution with one degree of freedom which—in the present context—is usually called a Porter-Thomas distribution [2,38]. Writing

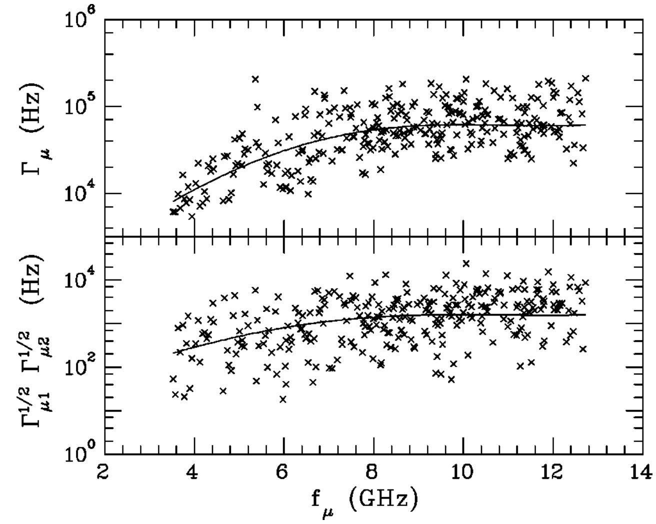

FIG. 3. The total widths (upper figure) and the square root of the strengths (lower figure) versus the resonance frequency of the $\lambda = 0.300$ Limaçon billiard for one antenna combination. The full line is the polynomial of fifth order obtained from a fit to the total widths. All strengths are rescaled with this polynomial in order to remove their secular dependence on the frequency

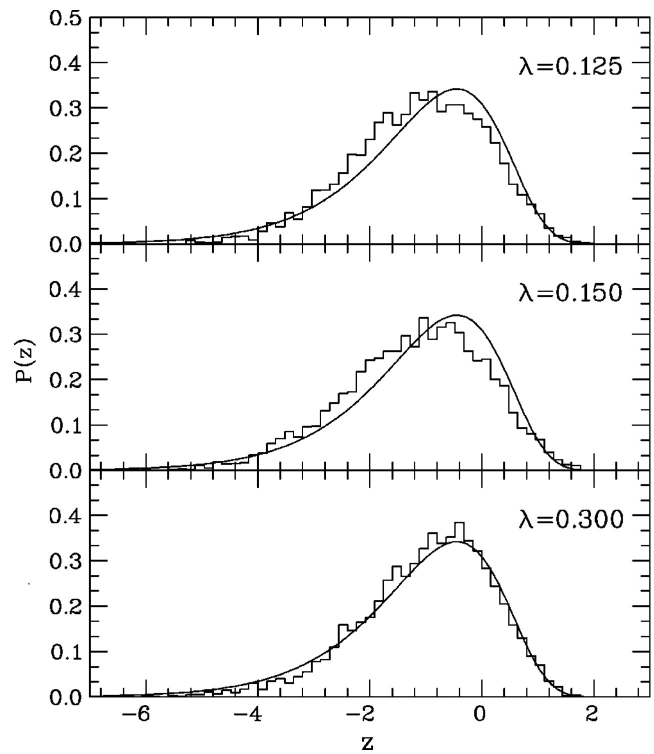

FIG. 4. The Distribution of the resonance strengths of the three Limaçon billiards. For each histogram the strength distributions of all six transmission spectra have been superimposed. While expected deviations from the GOE behavior (full line) are clearly visible for the billiards showing mixed dynamics ($\lambda = 0.125$ and $\lambda = 0.150$), the agreement between the RMT prediction, i.e., the K_0 distribution given in Eq. (12), and the measured strength distribution is good for the fully chaotic billiard ($\lambda = 0.300$) over more than six orders of magnitude.

$$t_a = \Gamma_{\mu a}, \tag{4}$$

the Porter-Thomas distribution reads

$$P_{\mathrm{PT}}(t_a|\tau_a)\mathrm{d}t_a = (2\pi t_a/\tau_a)^{-1/2}\exp\left(-\frac{t_a}{2\tau_a}\right)\frac{\mathrm{d}t_a}{\tau_a}. \tag{5}$$

Here, the parameter τ_a is the expectation value

$$\tau_a = \int_0^\infty t_a P_{\mathrm{PT}}(t_a|\tau_a)\mathrm{d}t_a \tag{6}$$

of t_a. It depends on the channel a under consideration, that is, the experimental data have to be evaluated for each antenna separately. Note that in Eq. (5) we use the notation of conditional distributions. The vertical bar separates the arguments of P into the random variable (to the left) and the parameters (to the right). For any value of the parameters the conditional distributions are normalized to unity.

As outlined in Sec. II, transmission measurements provide a direct access to the products of two partial widths, that is, the strength of a resonance. If the partial widths $\Gamma_{\mu a}$ and $\Gamma_{\mu b}$ both follow a Porter-Thomas distribution, their product has a so-called K_0-distribution,

$$P(y)\mathrm{d}y = \int_0^\infty \mathrm{d}t_a \int_0^\infty \mathrm{d}t_b P_{\mathrm{PT}}(t_a|\tau_a)P_{\mathrm{PT}}(t_b|\tau_b)\,\delta(y - t_a t_b)\mathrm{d}y$$

$$= \frac{K_0\left(\sqrt{\frac{y}{\tau_a\tau_b}}\right)}{\pi\sqrt{\frac{y}{\tau_a\tau_b}}}\frac{\mathrm{d}y}{\tau_a\tau_b}. \tag{7}$$

Here, K_0 is a Bessel function of imaginary argument [39]. The expression Eq. (7) is normalized to unity and the expectation value of y is $\tau_a\tau_b$. The product of expectation values

$$\tau_a\tau_b = \overline{\Gamma_{\mu a}}\;\overline{\Gamma_{\mu b}} \tag{8}$$

$$= \overline{\Gamma_{\mu a}\Gamma_{\mu b}} \text{ for } a \neq b \tag{9}$$

depends on the combination (a,b) of antennae. We estimated it by the experimental average

$$\tau_a\tau_b = N_{ab}^{-1}\sum_{\mu=1}^{N_{ab}} \Gamma_{\mu a}\Gamma_{\mu b} \tag{10}$$

of the N_{ab} available products of partial widths.

Since the distribution in Eq. (7) diverges for $y \to 0$, we follow [40] and transform it to the logarithmic variable

$$z = \log_{10}\left(\frac{y}{\tau_a\tau_b}\right). \tag{11}$$

This yields

$$P(z)\mathrm{d}z = \frac{\ln(10)}{\pi}10^{z/2}K_0(10^{z/2})\mathrm{d}z. \tag{12}$$

For each Limaçon billiard the histogram shown in Fig. 4 was obtained by superimposing the distributions of all six com-

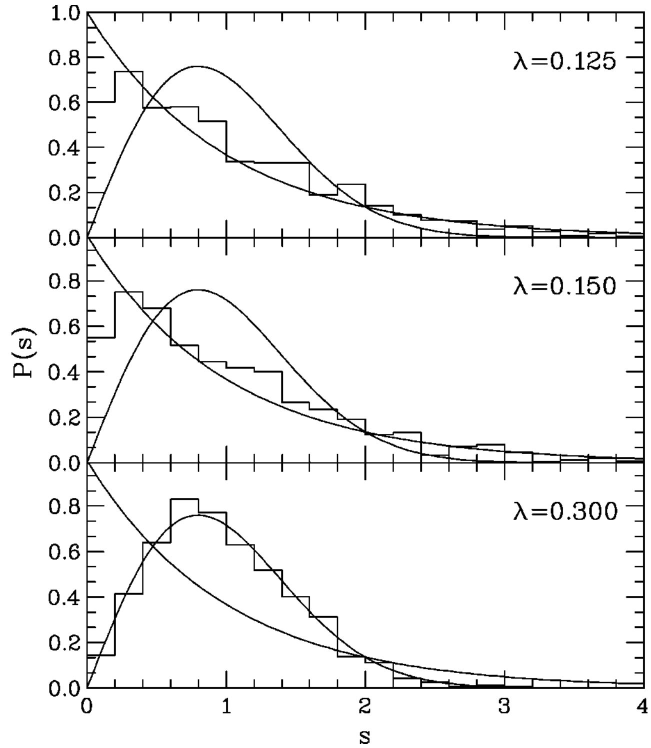

FIG. 5. The NNSDs for the three billiards from the family of the Limaçons. For the chaotic billiard (λ=0.300) the distribution coincides with the Wigner distribution, i.e., with that of random matrices from the GOE, while the two other billiards show a behavior in between GOE and Poisson statistics, see [17].

binations of antennae. The strength distributions of the two billiards with a mixed classical dynamics deviates from GOE behavior, while we find good agreement for the chaotic billiard. For comparison, we show in Fig. 5 the corresponding NNSD of the eigenvalues obtained by evaluating for each billiard the spectra of all antenna combinations. For λ =0.125, 0.150 the NNSD clearly deviates from the NNSD for random matrices from the GOE, that is, the so-called Wigner distribution, whereas for λ=0.300 the agreement is very good. Hence, we observe exactly the same behavior as for the strength distributions. However, there is one important difference, namely, while the spectral properties of regular systems generically have a Poissonian statistics, and there exist interpolating formulas for the mixed systems [17], there still is no general theory for the properties of the wave functions of such systems.

Still, even for the chaotic billiard, we observe small deviations between the measured strength distribution and the K_0 distribution at z values smaller than $z \simeq -3$. These are due to the experimental threshold of detection for narrow resonances and resonances with small strengths. It is taken into account in the theoretical description by normalizing the Porter-Thomas distribution to unity in the range of observable data. This procedure is equivalent to introducing a sharp cutoff into the Porter-Thomas distribution as lately discussed in [41]. Accordingly, $P_{\rm PT}(t_a|\tau_a)$ in Eq. (5) is replaced by

$$P_{\rm PT}(t_a|\tau_a,x_a)\mathrm{d}t_a = \frac{1}{\mathcal{N}(x_a)}\frac{\exp\left(-\frac{t_a}{2\tau_a}\right)}{\sqrt{2\pi t_a/\tau_a}}\Theta(t_a - x_a\tau_a)\frac{\mathrm{d}t_a}{\tau_a}, \tag{13}$$

$$\mathcal{N}(x_a) = \int_0^\infty \frac{\exp\left(-\frac{x}{2}\right)}{\sqrt{2\pi x}}\Theta(x - x_a)\mathrm{d}x \equiv \mathrm{erfc}\left(\sqrt{\frac{x_a}{2}}\right). \tag{14}$$

Here, $\Theta(x)$ is the step function. The parameter x_a denotes the threshold of detection. It depends on the channel a under consideration. Note that for $x_a \neq 0$ the quantity τ_a no longer equals the expectation value of t_a, but equals the ratio

$$\tau_a = \frac{\int_0^\infty t_a P_{\rm PT}(t_a|\tau_a)\mathrm{d}t_a}{\int_0^\infty t_a P_{\rm PT}(t_a|\tau_a = 1)\mathrm{d}t_a}. \tag{15}$$

By virtue of Eq. (13) the distribution of the product of two partial widths defined in Eq. (7) becomes

$$P(y|x_a,x_b)\mathrm{d}y = \int_0^\infty \mathrm{d}t_a \int_0^\infty \mathrm{d}t_b P_{\rm PT}(t_a|\tau_a,x_a)P_{\rm PT}(t_b|\tau_b,x_b) \times \delta(y - t_a t_b)\mathrm{d}y. \tag{16}$$

This distribution parametrically depends on both threshold parameters x_a and x_b. Note that it does not depend on τ_a and τ_b, when normalizing y to its expectation value.

Since in the experiment the threshold of detection is not sharp, an even more subtle analysis is appropriate, namely, the step function entering Eqs. (13) and (14) has to be replaced by a smooth step function,

$$\Theta_\epsilon(x) = \frac{1}{2}\left(1 + \frac{2}{\sqrt{\pi}}\int_0^{x/\sqrt{2}\epsilon} e^{-y^2}\mathrm{d}y\right). \tag{17}$$

Note that the normalization resulting from Eq. (14) can no longer be expressed in a closed form.

The threshold parameters x_a, x_b and the diffuseness ϵ have been determined for each antennae combination from a fit of the distribution Eq. (16) to the experimental distributions $P_{\rm exp}(y)$. Technically, this amounts to a search of that set of parameter values x_a, x_b and ϵ, for which the generalized entropy [38]

$$S = -\int P_{\rm exp}(y)\ln\left(\frac{P_{\rm exp}(y)}{P(y|x_a,x_b)}\right)\mathrm{d}y \tag{18}$$

is maximized. It turned out that the parameter ϵ can be chosen the same for all antenna combinations.

Here, the experimental distribution $P_{\rm exp}(y)$ is not a continuous probability density but rather a suitable histogram. Except for binning the data, the maximum entropy procedure is equivalent to the method of maximum likelihood [42]. In Fig. 6 we show the distribution obtained for one of the antenna combinations and for comparison the corresponding

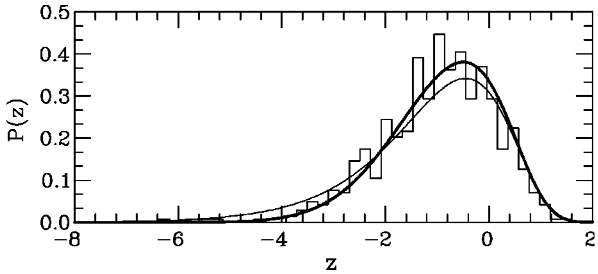

FIG. 6. A comparison of the experimental strength distribution of the resonances for one antenna combination in the chaotic Limaçon billiard (histogram) with the theoretical prediction (thick line) including a threshold of detection [Eq. (16)]. The threshold parameters and the parameter for the smooth cutoff were determined by a fit of the theoretical to the experimental curve to $x_a = x_b = 0.0057$ and $\epsilon = 0.0075$. The thin line shows the K_0 distribution Eqs. (7) and (12), i.e., the RMT prediction for chaotic systems with no threshold of detection.

experimental distribution. In this example the resulting values for the fit parameters are $\epsilon = 0.0075$, and $x_a = x_b = 0.0057$; the latter are identical within the numerical accuracy. Now the agreement between the theoretical curve and the experimental result has improved considerably.

From these results we may conclude that the deviations from the RMT behavior observed for z smaller than $z \simeq -3$ indeed are due to the experimental threshold of detection. In the present example the deviations are small, because the strength distribution already is close to zero for these values of z. For two coupled chaotic systems, or generally chaotic systems with one broken symmetry [13,38], however, this is not the case. There, the probability that the strengths take a value below the experimental threshold, that is, below $z \simeq -3$, is large and it is thus essential to include the experimental threshold of detection in the theoretical description. Experiments on spectral properties of two coupled chaotic microwave billiards have been performed [43]. In a forthcoming publication, we shall present our results on the corresponding strength distributions.

IV. CONCLUSION

In the present work we experimentally study statistical properties of the partial widths for three different billiards from the family of the Limaçons. Two of them have a mixed classical dynamics, one is chaotic. We measured transmission spectra, thereby obtaining products of two partial widths from the line shape of the resonances in the spectra. For a comparison with RMT we derived an analytic expression for the distribution of the products of two Porter-Thomas distributed random variables. Furthermore, we took into account the unavoidable experimental threshold of detection. As a result, we obtained a good agreement between the RMT prediction and the experimental distribution in the case of the chaotic Limaçon billiard, while we find deviations for the billiards with a mixed classical dynamics. For the strength distribution of the latter no theoretical model is available. In a subsequent publication we plan to use the strength distribution for the experimental study of the effect of partial symmetry breaking on the distribution of wave function components with two coupled chaotic microwave billiards. As outlined above, in such systems the treatment of the experimental detection threshold is of much greater importance than in the present work.

ACKNOWLEDGMENTS

This work has been supported by the DFG within SFB 634. We thank T. Guhr for several discussions and many hints and G. E. Mitchell for his continued interest in our experiments.

[1] O. Bohigas, M. J. Giannoni, and C. Schmit, Phys. Rev. Lett. **52**, 1 (1984).
[2] C. E. Porter, *Statistical Theories of Spectra: Fluctuations* (Academic, New York, 1965).
[3] M. L. Mehta, *Random Matrices*, 2nd ed. (Academic, San Diego, 1991).
[4] T. A. Brody, J. Flores, J. B. French, P. A. Mello, A. Pandey, and S. S. M. Wong, Rev. Mod. Phys. **53**, 385 (1981).
[5] T. Guhr, A. Müller-Groeling, and H. A. Weidenmüller, Phys. Rep. **299**, 189 (1998).
[6] N. Rosenzweig and C. E. Porter, Phys. Rev. **120**, 1698 (1960); H. S. Camarda and P. D. Georgopulos, Phys. Rev. Lett. **50**, 492 (1983); V. V. Flambaum, A. A. Gribakina, G. F. Gribakin, and M. G. Kozlov, Phys. Rev. A **50**, 267 (1994); G. Wunner, U. Woelk, I. Zech, G. Zeller, T. Ertl, F. Geyer, W. Schweitzer, and H. Ruder, Phys. Rev. Lett. **57**, 3261 (1986).
[7] E. Haller, H. Köppel, and L. S. Cederbaum, Chem. Phys. Lett. **101**, 215 (1983); T. Zimmermann, H. Köppel, and L. S. Cederbaum, J. Chem. Phys. **91**, 3934 (1989); D. M. Leitner, H. Köppel, and L. S. Cederbaum, J. Chem. Phys. **104**, 434 (1996); A. Delon, R. Jost, and M. Lombardi, J. Chem. Phys. **95**, 5701 (1991); B. Dietz, M. Lombardi, and T. H. Seligman, Ann. Phys. (N.Y.) **312**, 441 (2004); J. P. Pique, Y. Chen, R. W. Field, and J. L. Kinsey, Phys. Rev. Lett. **58**, 475 (1987).
[8] J. B. Garg, J. Rainwater, J. S. Petersen, W. W. Havens, Jr., Phys. Rev. **134**, B985 (1964); R. U. Haq, A. Pandey, and O. Bohigas, Phys. Rev. Lett. **48**, 1086 (1982); A. Y. Abul-Magd and H. A. Weidenmüller, Phys. Lett. **162B**, 223 (1985); Nucl. Phys. A **454**, 109 (1986); Nucl. Phys. A **481**, 189 (1988); G. E. Mitchell, E. G. Bilpuch, P. M. Endt, and J. F. Shriner, Jr., Phys. Rev. Lett. **61**, 1473 (1988); S. Raman, T. A. Walkiewicz, S. Kahane, E. T. Jurney, J. Sa, Z. Gàcsi, J. L. Weil, K. Allaart, G. Bonsignori, and J. F. Shriner, Jr., Phys. Rev. C **43**, 521 (1991); J. F. Shriner, Jr., E. G. Bilpuch, P. M. Endt, and G. E. Mitchell, Z. Phys. A **335**, 393 (1990); A. Y. Abul-Magd and M. H. Simbel, J. Phys. G **22**, 1043 (1996); **24**, 576 (1998); J. D. Garrett, J. Q. Robinson, A. J. Foglia, and H.-Q. Jin, Phys. Lett. B **392**, 24 (1997); J. F. Shriner, C. A. Grossmann, and G.

E. Mitchell, Phys. Rev. C **62**, 054305 (2000).
[9] C. M. Marcus, A. J. Rimberg, R. M. Westervelt, P. F. Hopkins, and A. C. Gossard, Phys. Rev. Lett. **69**, 506 (1992).
[10] V. Pascalutsa, Eur. Phys. J. A **16**, 149 (2003).
[11] H.-J. Stöckmann, *Quantum Chaos: An Introduction* (Cambridge University Press, Cambridge, 1999).
[12] A. Richter, in: *Emerging Applications of Number Theory, The IMA Volumes in Mathematics and its Applications*, Vol. 109, edited by D. A. Hejhal, J. Friedman, M. C. Gutzwiller, and A. M. Odlyzko (Springer, New York, 1999), p. 479.
[13] R. Weaver, J. Acoust. Soc. Am. **85**, 1005 (1989); P. Bertelsen, C. Ellegaard, T. Guhr, M. Oxborrow, and K. Schaadt, Phys. Rev. Lett. **83**, 2171 (1999); A. Andersen, C. Ellegaard, A. D. Jackson, and K. Schaadt, Phys. Rev. E **63**, 066204 (2001).
[14] V. Doya, O. Legrand, F. Mortessagne, and C. Miniatura, Phys. Rev. Lett. **88**, 014102 (2002); J. Dingjan, E. Altewischer, M. P. van Exter, and J. P. Woerdman, Phys. Rev. Lett. **88**, 064101 (2002).
[15] A. Y. Abul-Magd, H. L. Harney, M. H. Simbel, and H. A. Weidenmüller, Phys. Lett. B **579**, 278 (2004).
[16] J. Enders, T. Guhr, A. Heine, P. von Neumann-Cosel, V. Yu. Ponomarev, A. Richter, and J. Wambach, Nucl. Phys. A **741**, 3 (2004).
[17] H. Rehfeld, H. Alt, C. Dembowski, H.-D. Gräf, R. Hofferbert, H. Lengeler, and A. Richter, Nonlinear Phenom. Complex Syst. (Dordrecht, Neth.) **2**, 44 (1999).
[18] C. Dembowski, H.-D. Gräf, A. Heine, T. Hesse, H. Rehfeld, and A. Richter, Phys. Rev. Lett. **86**, 3284 (2001).
[19] H. Rehfeld, C. Dembowski, H.-D. Gräf, A. Heine, R. Hofferbert, and A. Richter, Physica E (Amsterdam) **9**, 518 (2001).
[20] M. Robnik, J. Phys. A **16**, 3971 (1983).
[21] A. Bäcker and R. Schubert, J. Phys. A **35**, 527 (2002); H. R. Dullin and A. Bäcker, Nonlinearity **14**, 1673 (2001); A. Bäcker and H. R. Dullin, J. Phys. A **30**, 1991 (1997); A. Bäcker, F. Steiner, and P. Stifter, Phys. Rev. E **52**, 2463 (1995).
[22] J. D. Jackson, *Classical Electrodynamics* (Wiley, New York, 1962).
[23] O. Bohigas, J. Gianonni, and C. Schmit, in *Quantum Chaos and Statistical Nuclear Physics*, edited by T. H. Seligman and H. Nishioka (Springer, Berlin, 1986).
[24] H.-J. Stöckmann and J. Stein, Phys. Rev. Lett. **64**, 2215 (1990).
[25] S. Sridhar, Phys. Rev. Lett. **67**, 785 (1991).
[26] H.-D. Gräf, H. L. Harney, H. Lengeler, C. H. Lewenkopf, C. Rangacharyulu, A. Richter, P. Schardt, and H. A. Weidenmüller, Phys. Rev. Lett. **69**, 1296 (1992).
[27] H. Alt, H.-D. Gräf, H. L. Harney, R. Hofferbert, H. Lengeler, A. Richter, P. Schardt, and H. A. Weidenmüller, Phys. Rev. Lett. **74**, 62 (1995).
[28] C. Dembowski, H.-D. Gräf, A. Heine, R. Hofferbert, H. Rehfeld, and A. Richter, Phys. Rev. Lett. **84**, 867 (2000).
[29] C. Dembowski, H.-D. Gräf, R. Hofferbert, H. Rehfeld, A. Richter, and T. Weiland, Phys. Rev. E **60**, 3942 (1999).
[30] F. Beck, C. Dembowski, A. Heine, and A. Richter, Phys. Rev. E **67**, 066208 (2003).
[31] E. P. Wigner and L. Eisenbud, Phys. Rev. **72**, 29 (1947).
[32] A. M. Lane and R. G. Thomas, Rev. Mod. Phys. **30**, 257 (1958).
[33] E. P. Wigner, Am. J. Phys. **17**, 99 (1949).
[34] In general, a fit with the formula of Eq. (31) in [30] only provides the product of the partial widths unambiguously, not the individual partial widths $\Gamma_{\mu a}$ and $\Gamma_{\mu b}$.
[35] Unfortunately, there is a misprint in the two-level formula of the Appendix of [30]. However, it is not difficult to obtain the correct formula by proceeding as described in the text preceding this formula.
[36] H. Weyl, J. Reine Angew. Math. **141**, 1 (1912); **141**, 163 (1912). **143** 177 (1913).
[37] H. P. Baltes and E. R. Hilf, *Spectra of Finite Systems* (Bibliographisches Institut Mannheim, Mannheim, 1975).
[38] C. I. Barbosa, T. Guhr, and H. L. Harney, Phys. Rev. E **62**, 1936 (2000).
[39] I. S. Gradshteyn and I. M. Ryzhik, *Tables of Integrals, Series, and Products* (Academic, New York, 1980), Secs. 8.407 and 8.432.
[40] A. A. Adams, G. E. Mitchell, W. E. Ormand, and J. F. Shriner Jr, Phys. Lett. B **422**, 1 (1998).
[41] S. Åberg, A. Heine, G. E. Mitchell, and A. Richter, Phys. Lett. B **598**, 42 (2004).
[42] H. L. Harney, *Bayesian Inference—Parameter Estimation and Decisions* (Springer Verlag, Heidelberg 2003), p. 26.
[43] H. Alt, C. I. Barbosa, H.-D. Gräf, T. Guhr, H. L. Harney, R. Hofferbert, H. Rehfeld, and A. Richter, Phys. Rev. Lett. **81**, 4847 (1998).